International Journal of Solid Materials
Vol. 1, Issue 1, 2019, Pages 117-136
Published Online on August 16, 2019

http://jyotiacademicpress.org

OPTIMUM DESIGN OF SUNKEN REINFORCED COMPARTMENTS UNDER BUCKLING CONDITION

MOSTAFA OMIDI-BIDGOLI and NIMA AMIRI

Department of Mechanical Engineering
Islamic Azad University
Badroud Branch
Badroud
Iran
e-mail: mostafaomidibidgoli@gmail.com

School of Mechanical Engineering
Sharif University of Technology
Tehran
Iran
e-mail: nimaamiri25@gmail.com

Abstract

Today, increasing the lifetime and improving the performance of structures through design and optimization, especially in marine structures, has become significantly important. Marine structures are divided into two groups of onshore and offshore structures. Marine structures are used in most cases inside the water and sea. These marine structures are divided into two categories: floating or sunken in water. One of the important parameters in the design of sunken structures is determining the critical load resulting from the buckling of walls, which can cause damage to structural. In this paper, three rectangular aluminum and steel compartments considering different conditions and sizes were modelled using design analytical methods. Then, different finite

Keywords and phrases: optimization, buckling, sunken reinforced compartments, marine structure, finite element simulation.

Communicated by Kazem Reza Kashyzadeh.

Received February 23, 2019; Revised March 15, 2019

element analysis were done and the compartments have been optimized in order to reduce the weight of the structure. Finally, the buckling results of three types of rectangular reinforced compartments were calculated and were compared with each other. The results shown that the stress calculated using analytical method are in good agreement with the results of finite element analysis. Also weight of the compartment is reduced by utilizing the reinforced conductors while respecting the design principles and the minimum thickness are considered.

1. Introduction

There are different types of pressure problems in various industries that have the potential to cause irreparable damages. One of these kinds of problems is to reinforce compartments by beam members to achieve higher strength against external loads. But, these structures are also subjected to local buckling, which should be carefully investigated at the design stage. A lot of researches has been done in this area. In 1744, Euler has described about the buckling of the columns for the first time. Afterthought, Brian has conducted the first theory tests for simple buckling [1]. The effect of slenderness ratio, influence of rectangular cube tanks on the local buckling and its general design for the application of aluminum alloys in a wide range of slenderness ratios have been studied [2, 3]. Rodriguez et al. [4] have evaluated the cyclic behaviour of rectangular reinforced concrete column under biaxial loading by utilizing experimental data. Avcar [5] has studied elastic buckling of steel columns under axial compression. Kervalishvili et al. [6] have presented a modified procedure for buckling of steel columns at elevated temperatures. Jiang et al. [7] have investigated the impact of two types of FCAW and SAW welding and different kind of heat treatment on the strength of high-strength steel (HSS) columns. The results indicated that applying appropriate heat treatment can increase the strength of the structure in the range of 3-7%. Moreover, a methodology has been present to test the HSS columns [8]. Schuman and Back [9] have done a series of different experiments on the rectangular flat plates under edge compression to assess strength. In addition, the strength of thin plates under compression condition has been reported [10]. The literature review indicated that the published results have been reported through analytical relationships for buckling are in good agreement with the experimental data under different loading. Among them can be pointed to the Graves Smith's which is about the final strength of the columns under the compressive load [11].

In the present study, a rectangular compartments made of different materials and sizes were analyzed by using FEM and analytical methods. Eventually, in order to reduce the weight of the structure, optimization was performed taking into account different variables such as thickness etc.

2. Model Description

Three compartments with different specifications were designed by using analytical method, utilizing finite element software, and applying available relationships and theories. The specifications of the rectangular compartment are reported in Table 1.

Table 1. Specifications of the rectangular compartment

External dimensions (mm)	Internal dimensions (mm)	Poisson ratio	Young's modulus (Gpa)	σ_y (Mpa)	Safety factor	Depth (m)	Body material
828*898*1551	768*838*1493	0.266	210	400	2.7	60	St60
		0.346	72.7	288	4	20	Al5083H321
		0.346	72.7	288	4	60	Al5083H321

3. Analytical Solution

The analytical solutions are used to design the compartments and calculate different parameters including deflection, maximum tension, and thicknesses based on Navier's solution [12, 13]:

$$p(x,\ y) = \sum_{m-1}^{\infty} \sum_{m-1}^{\infty} p_{mn} \sin \frac{m\pi x}{a} \sin \frac{n\pi y}{b} = p_0, \quad (1)$$

$$W(x,\ y) = \sum_{m-1}^{\infty} \sum_{m-1}^{\infty} a_{mn} \sin \frac{m\pi x}{a} \sin \frac{n\pi y}{b}, \tag{2}$$

where the a_{mn} coefficient is defined as follows:

$$a_{mn} = \frac{1}{\pi^4 D} \frac{P_{mn}}{\left[\left(\frac{m}{a}\right)^2 + \left(\frac{n}{b}\right)^2\right]^2}. \tag{3}$$

And the 2D stress components can be calculated:

$$\sigma_x = -\frac{EZ}{1-\nu^2}\left(\frac{\partial^2 w}{\partial x^2} + \nu \frac{\partial^2 w}{\partial y^2}\right), \tag{4}$$

$$\sigma_y = -\frac{EZ}{1-\nu^2}\left(\frac{\partial^2 w}{\partial y^2} + \nu \frac{\partial^2 w}{\partial x^2}\right), \tag{5}$$

$$\tau_{xy} = -\frac{EZ}{1-\nu^2}\left(\frac{\partial^2 w}{\partial x \partial y}\right). \tag{6}$$

For the constant load of P_0:

$$P_{mn} = \frac{4}{ab} \int_0^b \int_0^a P_0 \sin \frac{m\pi x}{a} \sin \frac{n\pi y}{b}\, dxdy$$

$$= \frac{4}{mn\pi^2}\left([(-1)^n - 1][(-1)^m - 1]\right). \tag{7}$$

This equation can be simplified as follows:

$$p_{mn} = \begin{cases} \dfrac{16 p_0}{mn\pi^2} & \text{if } m,\ n \text{ is not odd,} \\ 0 & \text{otherwise.} \end{cases} \tag{8}$$

By replacing the p_{mn} in the Equation (3):

$$a_{mn} = \frac{16 p_0}{mn\pi^2} * \frac{1}{mn\left[\left(\frac{m}{a}\right)^2 + \left(\frac{n}{b}\right)^2\right]^2}. \tag{9}$$

Afterthought, the parameter of a_{mn} is placed in the deflection equation:

$$W(x,\ y) = \sum \sum \frac{16P_0}{\pi^6 D} \frac{1}{mn\left[\left(\frac{m}{a}\right)^2 + \left(\frac{n}{b}\right)^2\right]^2} \sin\frac{m\pi x}{a} \sin\frac{n\pi y}{b}. \tag{10}$$

Since m and n are odd, τ_{xy} is always equal to zero. In the design stage, the Von Misses stress is used as the criterion. The characteristics of compartments made of different materials including steel and aluminum are presented in Table 2.

Table 2. Characteristics of compartments mate of different materials

Material	Von Misses stress	b	a	t	$w(x, y)$	τ_{xy}	σ_y	σ_x	Side
Steel	$\frac{1.92 * 10^5}{t^2}$	1522	798	36	2.3	0	$\frac{0.987 * 10^5}{t^2}$	$\frac{2.21 * 10^5}{t^2}$	1
	$\frac{2.12 * 10^5}{t^2}$	1522	868	37.8	3	0	$\frac{1.2 * 10^5}{t^2}$	$\frac{2.45 * 10^5}{t^2}$	2
	$\frac{1.14 * 10^5}{t^2}$	868	798	27.7	1.1	0	$\frac{1.07 * 10^5}{t^2}$	$\frac{1.2 * 10^5}{t^2}$	3
Aluminum (depth of 20m)	$\frac{0.646 * 10^5}{t^2}$	1522	798	30	3.5	0	$\frac{0.385 * 10^5}{t^2}$	$\frac{0.746 * 10^5}{t^2}$	1
	$\frac{0.724 * 10^5}{t^2}$	1522	868	31.7	4.6	0	$\frac{0.463 * 10^5}{t^2}$	$\frac{0.834 * 10^5}{t^2}$	2
	$\frac{0.404 * 10^5}{t^2}$	868	798	23.7	1.7	0	$\frac{0.384 * 10^5}{t^2}$	$\frac{0.421 * 10^5}{t^2}$	3
Aluminum (depth of 60m)	$\frac{1.94 * 10^5}{t^2}$	1522	798	51.9	2	0	$\frac{1.15 * 10^5}{t^2}$	$\frac{2.24 * 10^5}{t^2}$	1
	$\frac{2.17 * 10^5}{t^2}$	1522	868	54.9	2.7	0	$\frac{1.39 * 10^5}{t^2}$	$\frac{2.5 * 10^5}{t^2}$	2
	$\frac{1.21 * 10^5}{t^2}$	868	798	41	1	0	$\frac{1.15 * 10^5}{t^2}$	$\frac{1.26 * 10^5}{t^2}$	3

Considering the thicknesses obtained for each compartment, the maximum thickness is selected in design. Then, the characteristics of the equivalent reinforced plates are obtained with T and L-shaped reinforcements in respect of standards and minimizing the sum of weight. The number of reinforcements required is obtained as follows:

$$\frac{1}{12}bh^3 + bh(k - \frac{h}{2})^2 + n\left[I_{XX} + S(e_{XX} + h - k)^2\right] = \frac{1}{12}bt^3, \tag{11}$$

and

$$k = \frac{bh\frac{h}{2} + ns(e_{XX} + h)}{bh + ns}, \tag{12}$$

where b, h, and t represent the width, height, and thickness of sheet, respectively. The variable of n is number of reinforcement, I_X means the moment of inertia. Also, parameter of s is reinforcement cross-section and $e_{XX} = h - e_X$. Now, the number of reinforcements are obtained based on the calculations done for the T-shaped reinforcements. Properties of T-shaped reinforcements for different materials of the compartment are presented in Table 3. Final structures of reinforced compartments with T-shaped beam are shown in Figure 1.

Table 3. Properties of T-shaped reinforcements for different materials of the compartment

Material	B	Number of T	Property of T	h	T	Side
Steel	798	4	50	10	38	1
	868	4	50	10	38	2
	1522	7	50	10	38	3
Aluminum (depth of 20m)	798	3	80*80*9	10	55	1
	868	3	80*80*9	10	55	2
	1522	5	80*80*9	10	55	3
Aluminum (depth of 60m)	798	3	80*80*9	10	55	1
	868	3	80*80*9	10	55	2
	1522	5	80*80*9	10	55	3

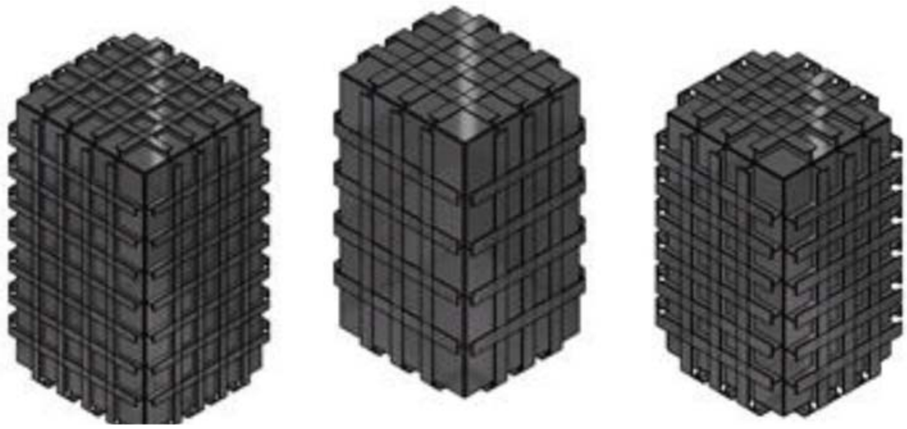

(a) (b) (c)

Figure 1. Final structures of reinforced compartments with T-shaped beam: (a) steel compartment, (b) aluminum compartment (depth of 20m), and (c) aluminum compartment (depth of 60m).

It is clear that the buckling phenomenon is one of the important issues which is to be attend in the shell & plate theories. Therefore, it seems that the buckling analysis should be done for all compartments considering different conditions. Equation (13) shows the general equation of the plate under loading:

$$D\Delta^2\Delta^2 W(x, y) = q(x, y) + N_X \frac{\partial^2 W}{\partial X^2} + N_Y \frac{\partial^2 W}{\partial Y^2} + 2N_{XY} \frac{\partial^2 W}{\partial X \partial Y}. \tag{13}$$

The boundary conditions are considered as:

$$N_X = N_Y = -N,$$

$$N_{XY} = 0,$$

$$q(x, y) = 0. \tag{14}$$

Since our plates have four hinge sides and using the above data, Navier's solution is followed:

$$\sum_{m=1}^{\infty}\sum_{n=1}^{\infty}\left[D\pi^4\left(\frac{m^2}{a^2}+\frac{n^2}{b^2}\right)^2-N\pi^2\left(\frac{m^2}{a^2}+\frac{n^2}{b^2}\right)\right]W_{mn}\sin\frac{m\pi x}{a}\sin\frac{n\pi y}{b}=0. \tag{15}$$

As a result, the critical load of buckling can be calculated in Equation (16):

$$N_{cr}=\frac{D\pi^4\left(\frac{m^2}{a^2}+\frac{n^2}{b^2}\right)^2}{\pi^2\left(\frac{m^2}{a^2}+\frac{n^2}{b^2}\right)}. \tag{16}$$

In the last step, the results of buckling calculations for different compartments are represented in Table 4.

Table 4. Buckling results obtained using analytical solution

Material	N_critical	n	m	b	a	t	No. sheet
Steel	3.01e7	1	1	868	798	38	1
	7.16e7	2	1	868	798	38	2
	1.8e7	1	1	1522	868	38	3
	3.2e7	2	1	1522	868	38	4
	2e7	1	1	1522	798	38	5
	3.4e7	2	1	1522	798	38	6
Aluminum (depth of 20m)	6.5e6	1	1	868	798	32	1
	1.5e7	2	1	868	798	32	2
	3.9e6	1	1	1522	868	32	3
	6.8e6	2	1	1522	868	32	4
	4.5e6	1	1	1522	798	32	5
	7.3e6	2	1	1522	798	32	6
Aluminum (depth of 60m)	3.2e7	1	1	868	798	55	1
	7.7e7	2	1	868	798	55	2
	1.9e7	1	1	1522	868	55	3
	3.4e7	2	1	1522	868	55	4
	3.2e7	1	1	1522	798	55	5
	3.7e7	2	1	1522	798	55	6

4. Finite Element Simulation

Stress analysis was done to examine the reliability coefficient of every three enclosures. The amount of force imposed from the hydrostatic pressure on each side and on the whole body is defined in accordance Equation (17):

$$P = \rho g h. \tag{17}$$

The equivalent Von Misses stress contours for various modes extracted from the FE software are demonstrated in Figure 2. Moreover, the results of the deflection of different structures are illustrated in Figure 3.

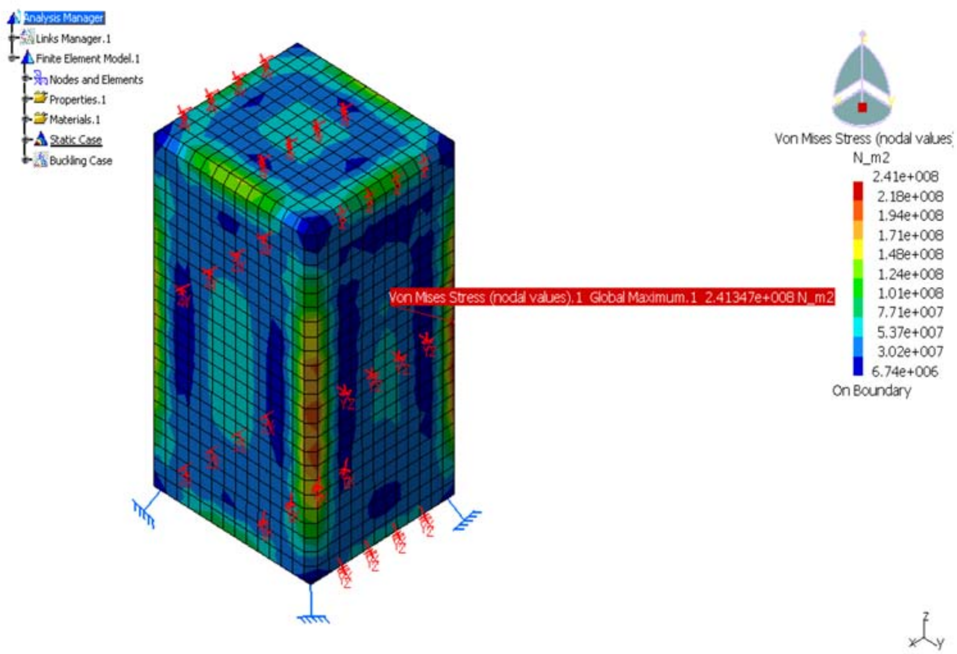
Analysis Manager
Links Manager.1
Finite Element Model.1
Nodes and Elements
Properties.1
Materials.1
Static Case
Buckling Case
Von Mises Stress (nodal values)
N_m2
2.41e+008
2.18e+008
1.94e+008
1.71e+008
1.48e+008
1.24e+008
1.01e+008
7.71e+007
5.37e+007
3.02e+007
6.74e+006
On Boundary
Von Mises Stress (nodal values).1 Global Maximum.1 2.41347e+008 N_m2

(a)

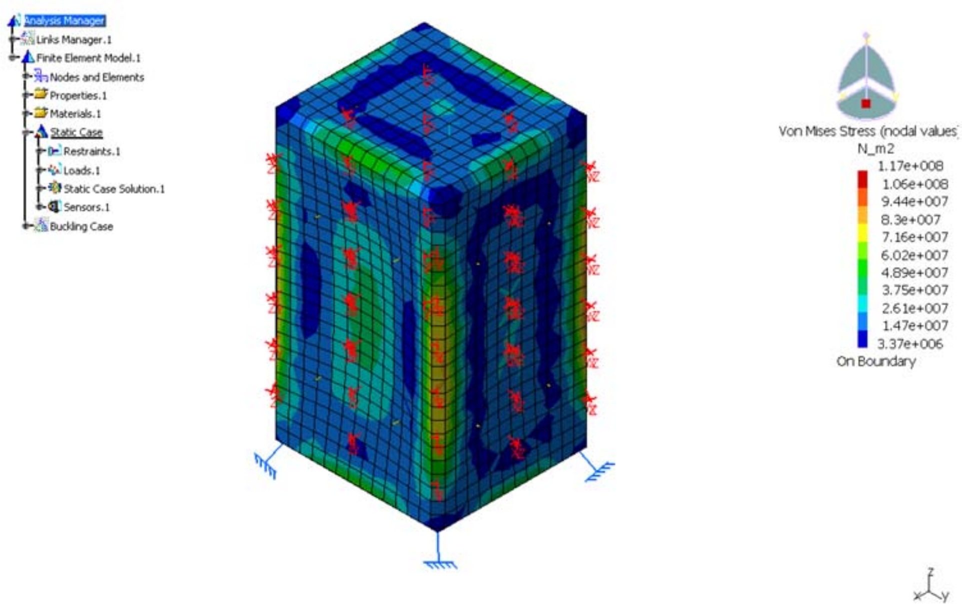
Analysis Manager
Links Manager.1
Finite Element Model.1
Nodes and Elements
Properties.1
Materials.1
Static Case
Restraints.1
Loads.1
Static Case Solution.1
Sensors.1
Buckling Case
Von Mises Stress (nodal values)
N_m2
1.17e+008
1.06e+008
9.44e+007
8.3e+007
7.16e+007
6.02e+007
4.89e+007
3.75e+007
2.61e+007
1.47e+007
3.37e+006
On Boundary

(b)

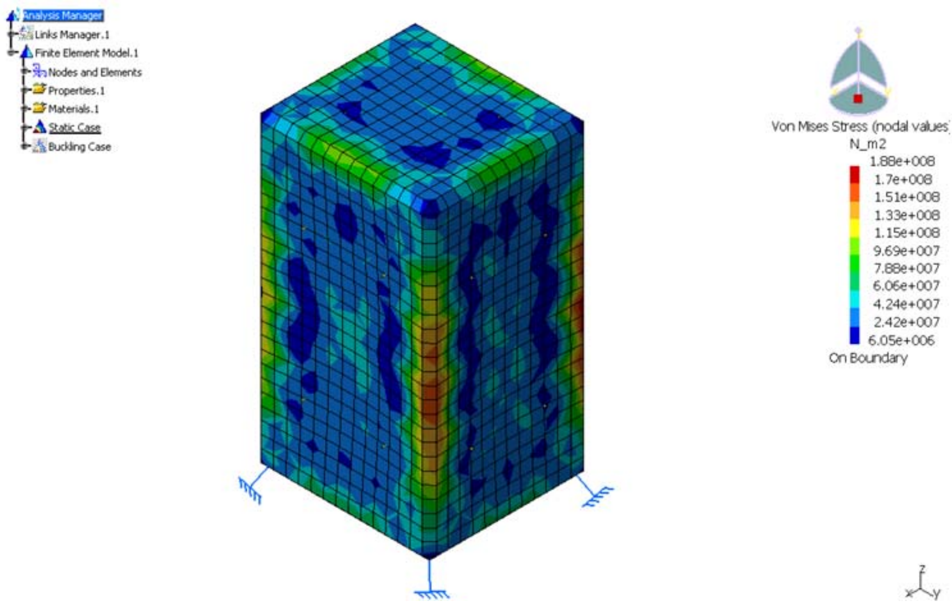

(c)

Figure 2. Contours of Von Misses stresses for various modes of compartments: (a) steel compartment, (b) aluminum compartment (depth of 20m), and (c) aluminum compartment (depth of 60m).

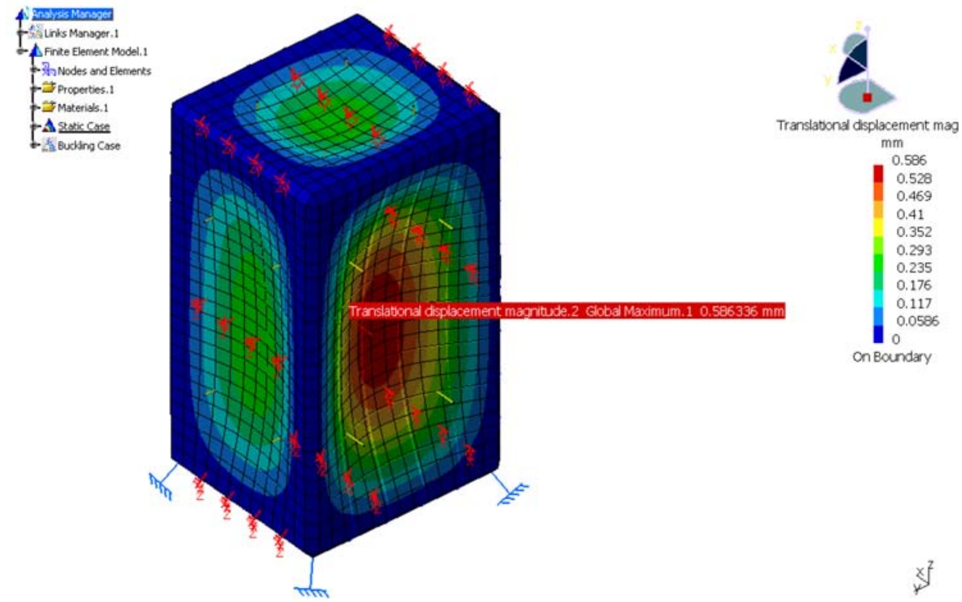
Analysis Manager
Links Manager.1
Finite Element Model.1
Nodes and Elements
Properties.1
Materials.1
Static Case
Buckling Case
Translational displacement mag
mm
0.586
0.528
0.469
0.41
0.352
0.293
0.235
0.176
0.117
0.0586
0
On Boundary
Translational displacement magnitude.2 Global Maximum.1 0.586336 mm

(a)

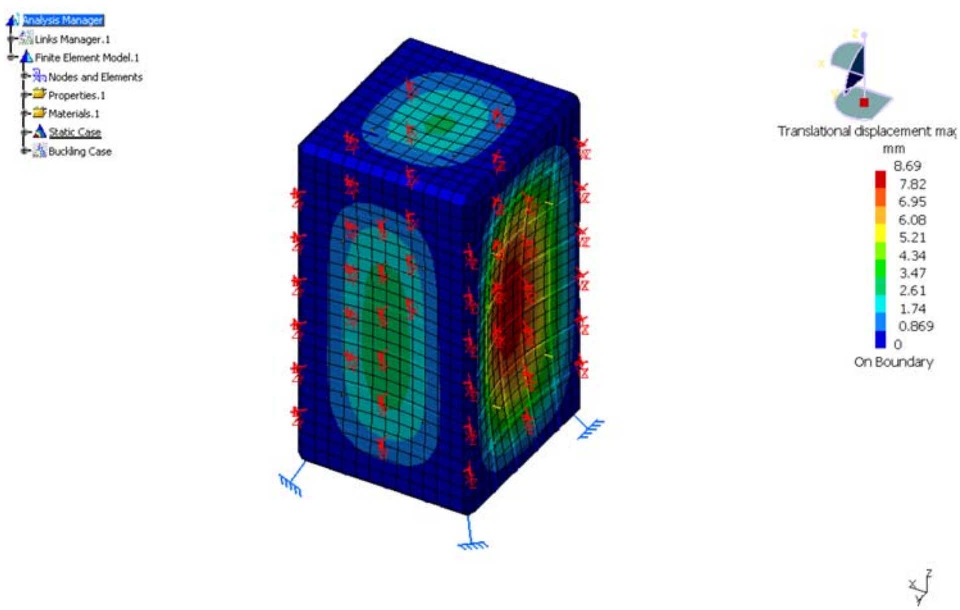
Analysis Manager
Links Manager.1
Finite Element Model.1
Nodes and Elements
Properties.1
Materials.1
Static Case
Buckling Case
Translational displacement mag
mm
8.69
7.82
6.95
6.08
5.21
4.34
3.47
2.61
1.74
0.869
0
On Boundary

(b)

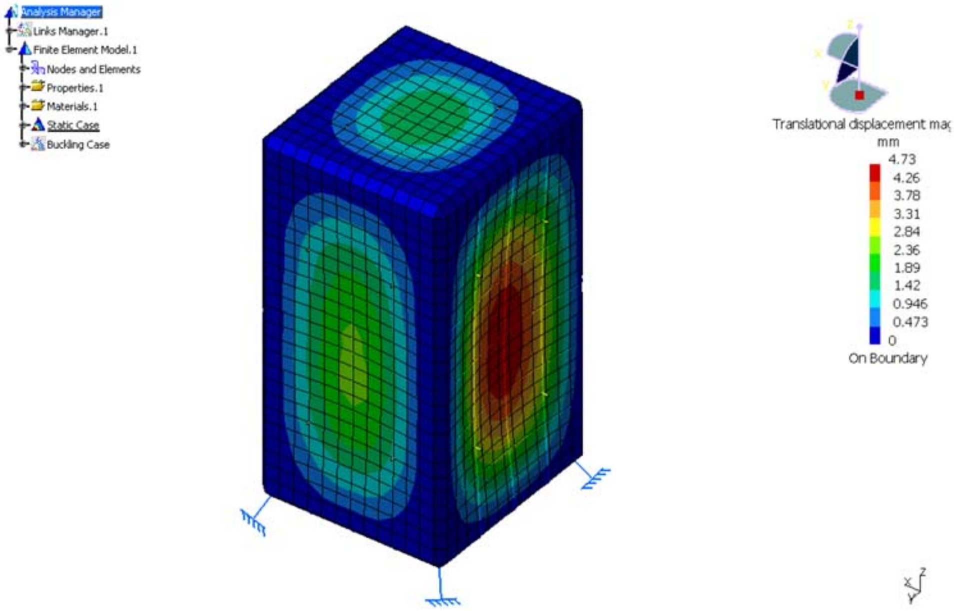

(c)

Figure 3. Deflection contours as FE results for various modes of compartments: (a) steel compartment, (b) aluminum compartment (depth of 20m), and (c) aluminum compartment (depth of 60m).

The results obtained from finite element analysis including critical stress and value of deformation are summarized in Table 5. More than this, the first three shape modes of buckling phenomenon for different materials are shown in Figure 4. The results indicated that the shape mode is independent of material. Hence, the corresponding images of the similar number of shape modes are same.

Table 5. Critical stress and deformation extracted from FEA

Compartment type	Max. deformation (mm)	Critical stress (Mpa)	Safety factor
St 60	0.586	241	3
Al + depth 20	8.69	117	2.4
Al + depth 60	4.73	188	2

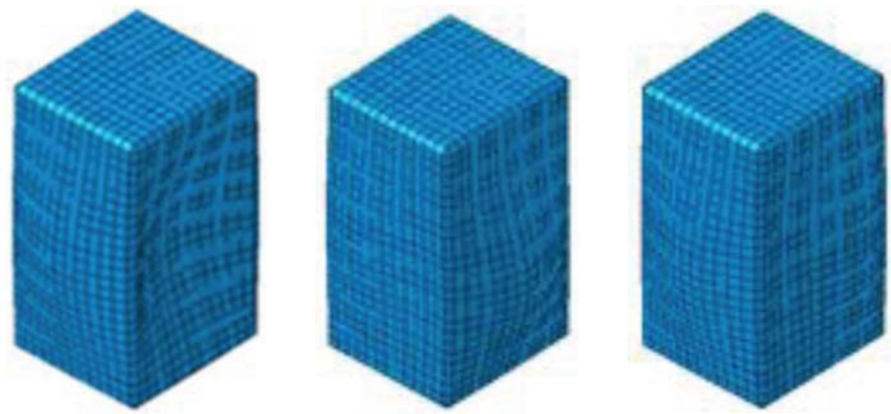

Mode shape I   Mode shape II   Mode shape III

Figure 4. The first three mode shapes of buckling of compartment.

Finally, the buckling factor (BF) is obtained for different cases of compartments, as reported in Table 6.

Table 6. Buckling factor for different cases of compartments

Mode No.	BF		
	Steel	Al + Depth 20	Al + Depth 60
1	179.99	12.259	23.474
2	288.64	18.950	37.018
3	307.52	21.164	38.438
4	316.34	22.921	43.353
5	407.86	28.474	54.950
6	436.16	30.11	56.925
7	464.74	33.113	60.156
8	480.94	34.016	60.847
9	499.73	34.953	64.814
10	536.31	35.862	65.657

5. Results and Discussion

In this stage of study, the optimization with an aim of weight reduction was performed to choose the best design among all of them. This process was performed by using the FE software features (ANSYS WORKBENCH) and the details of optimum designs are presented in Table 7. Also, stress analysis was conducted for all the optimized compartments and the FE results are depicted in Figure 5.

Table 7. Details of optimum design for different cases of compartments

Compartment type	Type of reinforced beam	Number of beams	Sheet thickness (mm)	Safety factor	Weight (kg)
Steel	50 T	4, 4, 7	10	3	1199
Al + Depth 20	40*80*7 T	3, 3, 4	12	2.83	305
Al + Depth 60	80*80*9 T	3, 3, 6	8	3.51	446

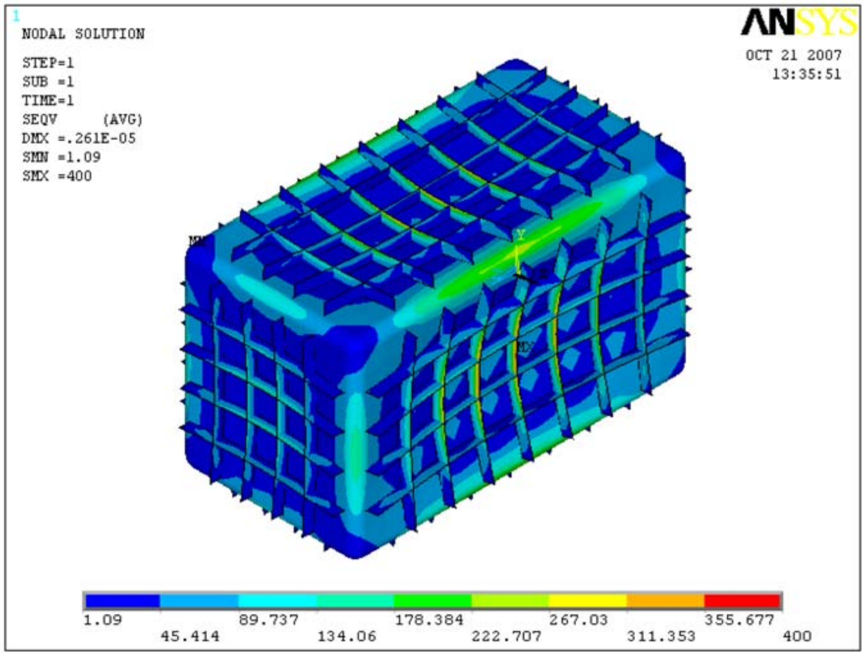
NODAL SOLUTION
STEP=1
SUB =1
TIME=1
SEQV (AVG)
DMX =.261E-05
SMN =1.09
SMX =400
ANSYS
OCT 21 2007
13:35:51
1.09
45.414
89.737
134.06
178.384
222.707
267.03
311.353
355.677
400

(a)

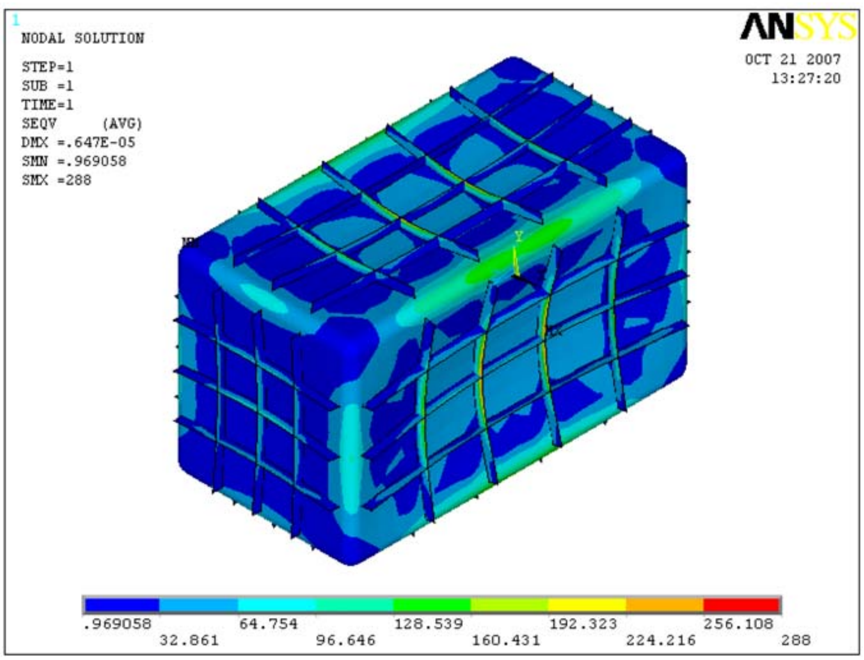
NODAL SOLUTION
STEP=1
SUB =1
TIME=1
SEQV (AVG)
DMX =.647E-05
SMN =.969058
SMX =288
ANSYS
OCT 21 2007
13:27:20
.969058
32.861
64.754
96.646
128.539
160.431
192.323
224.216
256.108
288

(b)

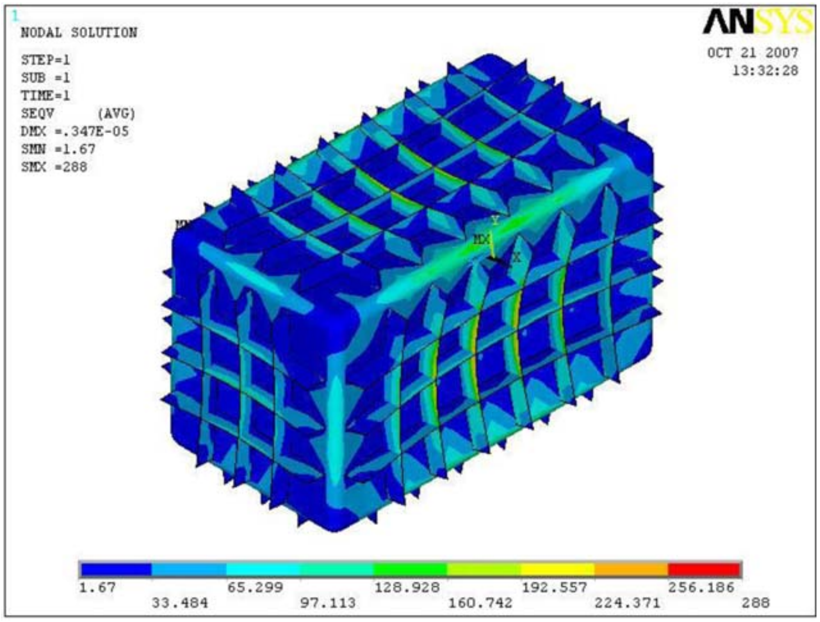

(c)

Figure 5. Results of stress analysis of optimized compartments made of different materials including: (a) steel compartment, (b) aluminum compartment (depth of 20m), and (c) aluminum compartment (depth of 60m).

6. Conclusion

The results of the research are as follows:

• According to the prevailing conditions, the best compartments have been designed. Because the weight of the compartment is reduced by utilizing the reinforced conductors while respecting the design principles and the minimum thickness are considered.

• The stress results calculated using analytical method are in good agreement with the results of finite element analysis.

• The final thicknesses computed against the load and local buckling had good and adequate strength. It seems that it can be used at arbitrary depths.

References

[1] A. C. Walker, A Brief Review of Plate Buckling Research, the Behavior of Thin-Walled Structures, Elsevier, London, 1984.

[2] P. P. Bijlaard and G. P. Fisher, Interaction of Column and Local Buckling in Compression Members, NACA Technical Note 2640, 1952.

[3] P. P. Bijlaard and G. P. Fisher, Column Strength of H-Sections and Square Tubes in the Post-Buckling Range of Component Plates, NACA Technical Note 2994, 1953.

[4] H. Rodrigues, A. Arêde, H. Varum and A. G. Costa, Experimental evaluation of rectangular reinforced concrete column behaviour under biaxial cyclic loading, Earthquake Engineering Structural Dynamics 42(2) (2013), 239-259.

DOI: https://doi.org/10.1002/eqe.2205

[5] M. Avcar, Elastic buckling of steel columns under axial compression, American Journal of Civil Engineering 2(3) (2014), 102-108.

DOI: https://doi.org/10.11648/j.ajce.20140203.17

[6] A. Kervalishvili and L. Talvik, Modified procedure for buckling of steel columns at elevated temperatures, Journal of Constructional Steel Research 127 (2016), 108-119.

DOI: https://doi.org/10.1016/j.jcsr.2016.07.008

[7] J. Jiang, J. Zhang, J. Liu, S. Chiew and C. K. Lee, Effect of welding and heat treatment on strength of high-strength steel columns, Journal of Constructional Steel Research 151 (2018), 238-252.

DOI: https://doi.org/10.1016/j.jcsr.2018.09.027

[8] K. J. R. Rasmussen and G. J. Hancock, Tests of high strength steel columns, Journal of Constructional Steel Research 34(1) (1995), 27-52.

DOI: https://doi.org/10.1016/0143-974X(95)97296-A

[9] L. Schuman and G. Back, Strength of Rectangular Flat Plates Under Edge Compression, NACA Report No. 356, 1930.

[10] T. Karman, E. E. Sechler and L. H. Donnel, The strength of thin plates in compression, Trans ASME (1932).

[11] T. R. Graves Smith, The Ultimate Strength of Locally Buckled Columns of Arbitrary Length, the Thin-Walled Steel Constructions, Symposium University College, Swansea, 1967.

[12] W. Flugge, Stresses in Shells, Julius Springer, Berlin, 1960.

DOI: https://doi.org/10.1007/978-3-662-01028-0

[13] S. Timoshenko and S. Woinowsky-Krieger, Theory of Plates and Shells, McGraw-Hill Publishing Co., Inc., New York, N.Y., 1960.

■